

Linking Acoustic Communications and Network Performance: Integration and Experimentation of an Underwater Acoustic Network

Andrea Caiti, *Senior Member, IEEE*, Knut Grythe, *Member, IEEE*, Jens M. Hovem, Sérgio M. Jesus, *Member, IEEE*, Arne Lie, Andrea Munafò, *Member, IEEE*, Tor Arne Reinen, António Silva, and Friedrich Zabel

Abstract—Underwater acoustic networks (UANs) are an emerging technology for a number of oceanic applications, ranging from oceanographic data collection to surveillance applications. However, their reliable usage in the field is still an open research problem, due to the challenges posed by the oceanic environment. The UAN project, a European-Union-funded initiative, moved along these lines, and it was one of the first cases of successful deployment of a mobile underwater sensor network integrated within a wide-area network, which included above water and underwater sensors. This contribution, together with a description of the underwater network, aims at evaluating the communication performance, and correlating the variation of the acoustic channel to the behavior of the entire network stack. Results are given based on the data collected during the UAN11 (May 2011, Trondheim Fjord area, Norway) sea trial. During the experimental activities, the network was in operation for five continuous days and was composed of up to four Fixed NODes (FNOs), two autonomous underwater vehicles (AUVs), and one mobile node mounted on the supporting research vessel. Results from the experimentation at sea are reported in terms of channel impulse response (CIR) and signal-to-interference-plus-noise ratio (SINR) as measured by the acoustic modems during the sea tests. The performance of the upper network levels is measured in terms of round trip time (RTT) and probability of packet loss (PL). The analysis shows how the communication performance was dominated by variations in signal-to-noise ratio, and how this impacted the behavior of the whole network. Qualitative explanation of communication performance variations can be accounted, at least in the UAN11 experiment, by standard computation of the CIR and transmission loss estimate.

Manuscript received November 16, 2012; revised February 28, 2013 and June 21, 2013; accepted August 12, 2013. Date of publication September 06, 2013; date of current version October 09, 2013. This work was supported in part by the European Union under the FP7 Underwater Acoustic Network (UAN) Project under Grant 225669.

Associate Editor: J. Potter; Guest Editor: J. Preisig.

A. Caiti is with the Inter-university Center on Integrated Systems for the Marine Environment, Research Center E. Piaggio, University of Pisa, Pisa 56122, Italy (e-mail: andrea.caiti@dsea.unipi.it)

K. Grythe, A. Lie, and T. A. Reinen are with SINTEF, Trondheim N-7465, Norway (e-mail: knut.grythe@sintef.no; Arne.Lie@sintef.no; Tor.A.Reinen@sintef.no).

J. M. Hovem is with the Department of Electronics and Telecommunication, Norwegian University of Science and Technology (NTNU), Trondheim NO-7491, Norway (e-mail: jens.hovem@iet.ntnu.no).

S. M. Jesus, A. Silva, and F. Zabel are with the Institute for Systems and Robotics, University of Algarve, Faro 8005-139, Portugal (e-mail: sjesus@ualg.pt; asilva@ualg.pt; fredz@wireless.com.pt)

A. Munafò was with the Inter-university Center on Integrated Systems for the Marine Environment, Research Center E. Piaggio, University of Pisa, Pisa 56122, Italy. He is now with the NATO STO Center for Maritime Research and Experimentation (CMRE), La Spezia 19126, Italy (e-mail: munaf0@cmre.nato.int).

Color versions of one or more of the figures in this paper are available online at <http://ieeexplore.ieee.org>.

Digital Object Identifier 10.1109/JOE.2013.2279472

Index Terms—Autonomous systems, multiagent systems, underwater acoustics, underwater communication, wireless sensor networks.

I. INTRODUCTION

THE ongoing increase in reliability and performance of acoustic modem devices is paving the way to the development of mobile underwater sensor networks [1], [2], characterized by a number of autonomous sensing units, either fixed or mobile, by distributed sensing and data processing, and by adaptivity on the basis of locally sensed data. Underwater acoustic networks (UANs) are an emerging technology for oceanographic data collection, pollution monitoring, offshore exploration, and tactical surveillance applications. However, the transition from theoretical or proof-of-concept experiment to operational application in the underwater domain poses tougher challenges with respect to the terrestrial or aerial counterparts. The unique characteristics of the underwater acoustic channel make the efficient design of network models challenging, and their reliable implementation still an open research field. The major challenge in underwater application of autonomous cooperating sensing networks is still represented by node communication. In fact, the intrinsic limitations in bandwidth, time delay, and channel fluctuation, imposed by the physics of acoustic propagation, have constrained the reliable setup of communication infrastructures for sensor networks [3]–[5]. A theoretical overview of recent protocols for underwater networks is reported in [6], where Pompili and Akyildiz highlight the main drawbacks of most of the current acoustic network designs for robust and efficient UANs. Underwater acoustic networks are still characterized by very large propagation delays, extremely low point-to-point (P2P) data rates, high raw bit error rate (BER), and frequent disruption of the communication links. Furthermore, field examples of UANs with measured performance in the field are scarce. An initial attempt to establish a UAN was conducted in 1998 with the SeaWeb experiments [7], with the aim of improving acoustic modems, originally developed for P2P communications, for usage within UANs. During the same project, medium access control (MAC) and routing protocols were investigated for networks composed of underwater Fixed NODes (FNOs) and gateways. The SeaWeb experiments aimed at demonstrating the capability of UANs for surveillance operations. The experimental testing of an underwater network with mobile nodes

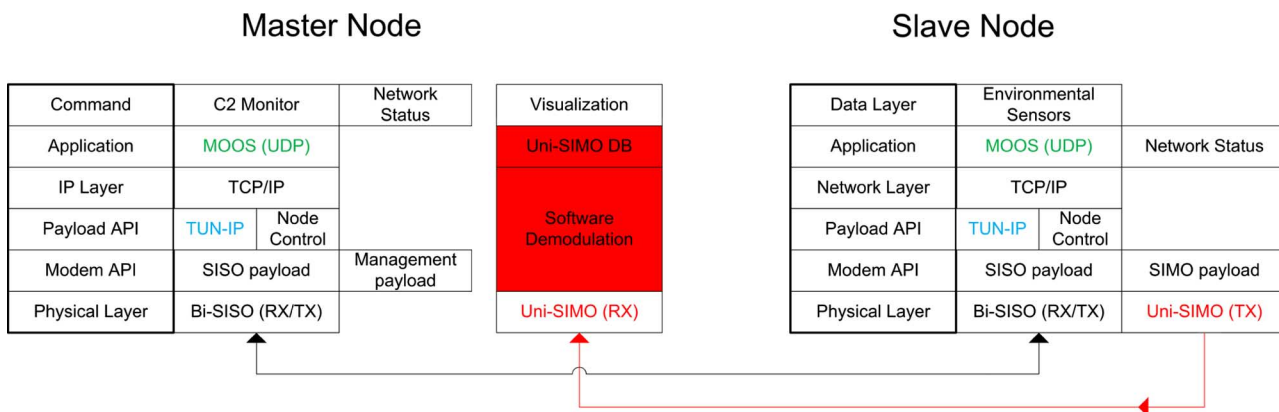


Fig. 2. Implementation of the network layers at master node (STU) and at slave nodes. The picture shows the difference on how the bi-SISO link was handled using the entire network stack, whereas the uni-SIMO link, capable of high data rate communications, is handled using a leaner and parallel structure to increase communication efficiency.

the CIR and the transmission loss changed between the nodes of the network as the oceanic conditions changed. Section VII is devoted to observations and remarks on the achieved communication performance. Finally, conclusions are drawn in Section VIII.

II. NETWORK STRUCTURE AND TOPOLOGY

The UANp network is a component of a wide area network, which includes above water and underwater sensors. The integration point between the underwater and above water parts of the system is represented by the subsurface telemetry unit (STU) connected to shore with a high bandwidth link (fiber optic cable), and which is both a part of the acoustic network and of a traditional wired communication infrastructure. The underwater network is composed of acoustically connected fixed and mobile nodes, which act both as communication nodes and as surveillance sensing nodes.

Figs. 1 and 2 show two levels of detail of the conceptual overview of the UANp network structure including the flow of data and information. The rest of the section describes the specific hardware and software used in the underwater network.

1) *UANp Physical Layer—The Acoustic Modems:* The physical layer of the UANp network is supported on the cNODE®Mini transponders model 34–180 provided by Kongsberg Maritime (KM, Kongsberg, Norway) and specifically adapted to the task (see a detailed description in [16]). The acoustic modems operate through a 180° beam pattern transducer at a center frequency $f = 25.6$ kHz, with a bandwidth $B = 8$ kHz, emitted power between 173 dB re 1 $\mu\text{Pa}@1\text{m}$, which was the most often used during the trials, and 190 dB re 1 $\mu\text{Pa}@1\text{m}$. The cNODE mini transponder uses binary phase-shift keying/quadrature phase-shift keying (BPSK/QPSK) signaling with a variable spreading factor direct sequence spread-spectrum (DSSS) modulation. The spreading factor can be as low as one to attain pure BPSK/QPSK (detailed technical information can be found in [17]).

The modems supported two types of acoustic traffic: normal network traffic that was transmitted via bidirectional single-input–single-output (bi-SISO) links (between individual

modems), and high priority, high data rate, traffic that could be exchanged using unidirectional links from each individual node directly toward a vertical line array of hydrophones located at the STU using a single-input–multiple-output (uni-SIMO) link. The uni-SIMO link does not pass via the main network stack, whereas it is handled using a leaner and parallel communication structure to increase the communication efficiency (see Fig. 2). The bi-SISO link, through which the modems operate with direct links or via multihops, can hence be used for routine message exchange within the network (e.g., monitoring of node status, environmental data exchange, etc.), whereas critical information (e.g., threat detection) can be transmitted using the high-priority uni-SIMO link to quickly reach the STU. The lower part of Fig. 1 shows the gateway node STU possible connection types [either bi-SISO, uni-SIMO, or logical tunnelling–Internet protocol (TUN–IP)] to the various nodes in the UANp network: two mobile nodes, MN1 and MN2, and two FNOs, FN1 and FN2.

The information bit rate (training and coding excluded) in bi-SISO mode was 200, 500, and 1600 b/s. Lower bit rates were based on a spread-spectrum technique, whereas turbo coding was used to reach the highest bit rate (not used in the sea trial). In uni-SIMO mode, the maximum information bit rate was 8000 b/s, using QPSK. The modems were able to provide an online CIR estimation exploiting training sequences available in every transmitted acoustic telegram, and to use this information to mitigate the intersymbolic interference (ISI). It should be pointed out that, at the physical level, KM modems use a slicing of data packets into telegrams which maximum size varies with the transmission rate, in this case, 50, 120, and 231 B of telegram size for 200, 500, and 1600 b/s bit rate, respectively.

Since the uni-SIMO link is a network transparent P2P connection, the focus of this paper will be on the bi-SISO network mode. More information on the uni-SIMO system implementation and results obtained during the 2010 sea trial (UAN10, Pianosa Island, Italy) can be found in [18].

2) *MAC and Routing Layers:* The lowest levels of the network were implemented directly on the modems digital signal

processing (DSP) board, and this included: a) MAC—implemented in the form of carrier sense multiple access/collision avoidance (CSMA/CA) and supplemented by request to send/clear to send (RTS/CTS) for initiating transmission to a particular node; and b) routing—a flooding algorithm allowed for network discovery at bootstrap and in presence of topology modification events (e.g., mobile nodes movement).

The network was hence able to support retransmissions at the physical layer to decrease the probability of PL, and was equipped with an addressing system for data packet switching and forwarding. Packets sent out in the water were repeated up to three times by the transmitter, if no acknowledgement was received from the next destination node. A ten-packet FIFO buffer queue was implemented between the modem application programming interface (API) and the TUN-IP (see Section II-A3) so as to handle packets to be transmitted. Overflow packets were discarded.

3) *UANp Network Upper Layers*: On top of the bi-SISO layer, the UANp stack was completed by an IP tunneling mechanism (TUN-IP layer, in blue in Fig. 1) to establish the IP connection among the nodes, by the user datagram protocol (UDP) as the transport protocol, and by the intervehicle secure-mission orientated operating suite (IS-MOOS) as the middleware level (in green in Fig. 1). IS-MOOS is a publish/subscribe system, based on the MOOS framework [19], which was used, in the UAN context, to include network security mechanisms, such as integrity, confidentiality, and authentication, and to create the network interface toward the applications. Details on the specific security methodologies used in UANp are reported in [11]. The use of UDP was motivated to reduce the communication overhead typical of connection-oriented protocols, such as TCP. However, this makes the protocol reliability dependent on lower network layers; for example, retransmission was handled at the physical level. Finally, the use of IP had the advantage of providing a standard interface toward the upper levels of the network.

Both IP and MOOS layers created a star-shaped network with the STU at the center (a gateway or a master node). In general, this might create a bottleneck for the network, since all the traffic must pass through this point, independently from the lower level configuration. In the case of the UANp network, though, due to its specific application (i.e., security and protection of critical infrastructures), this choice did not add a significant amount of overhead, since all the data had to go in any case to the C2 station, which was collocated with the STU. The C2 station in fact had the complete control over the network behavior (e.g., node status monitoring, WAN integration, operational missions determination). The C2 station presence in the network structure is depicted in purple in Fig. 1.

III. UAN11 SEA TRIAL: TRONDHEIM FJORD, MAY 2011

The UANp network described in Section II was deployed and tested during the UANp final sea trial, UAN11, which took place in May 2011 in the eastern part of Strindfjorden, 17 km from Trondheim, Norway. The area, with varying bathymetry

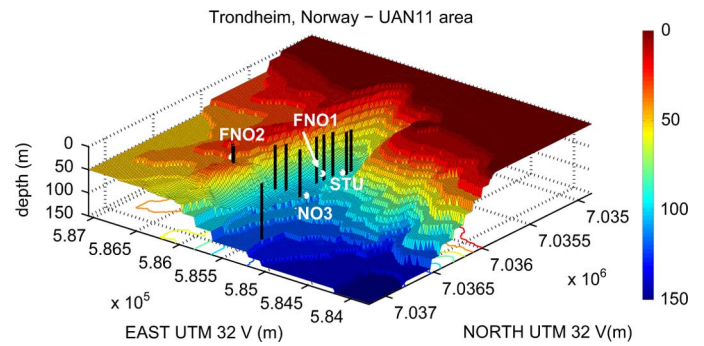


Fig. 3. UAN FNOs' location superimposed on the bathymetric map. Bathymetry was obtained first from multibeam echo sounder data from *R/V Gunnerus* collected on May 24, 2011, and as supplement depth information extracted from screen dumps of the Olex map system of the ship. CTD cast positions are displayed as vertical black lines at the corresponding locations.

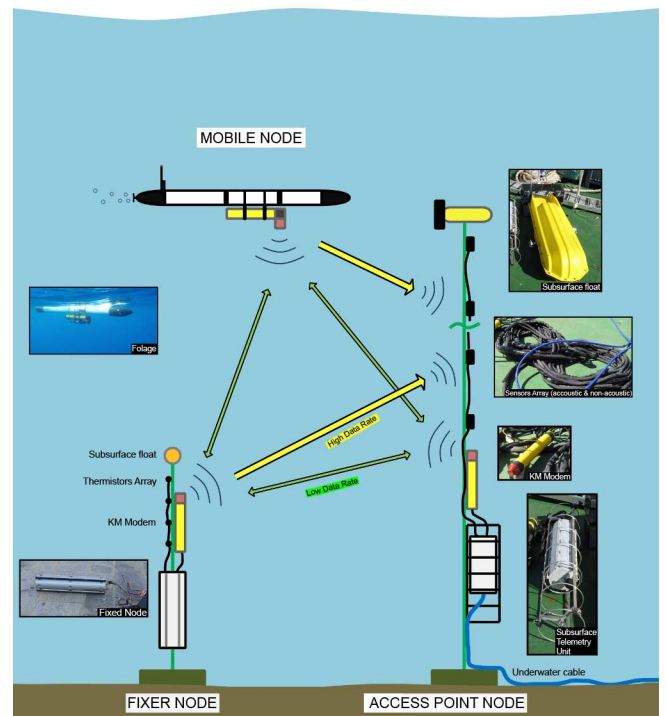


Fig. 4. UANp equipment: FNO composed of a vertical array of environmental sensors, a telemetry box, and a modem (bottom left); mobile node composed of an AUV and a modem (upper left); access point node (or STU gateway), made of a vertical line array of hydrophones, environmental sensors, a modem, and a shore connected telemetry box (right); green and yellow arrows represent bi-SISO and uni-SIMO links between nodes, respectively.

ranging from 40 to 150 m, is close to commercial and touristic routes, allowing to test the system in operative conditions. The deployed network (see Figs. 3 and 13) was composed of up to four FNOs including the gateway node (STU), and three mobile nodes: two AUVs of e-Folaga class [14] and one additional mobile node setup on the supporting research vessel (*R/V Gunnerus*) using a transducer located at 20-m depth. A fiber optic cable connected the underwater network to the C2 station, which integrated aerial and surface additional sensors and nodes. Fig. 4 shows the main equipment parts forming the UANp network and deployed during the UAN11 activities.

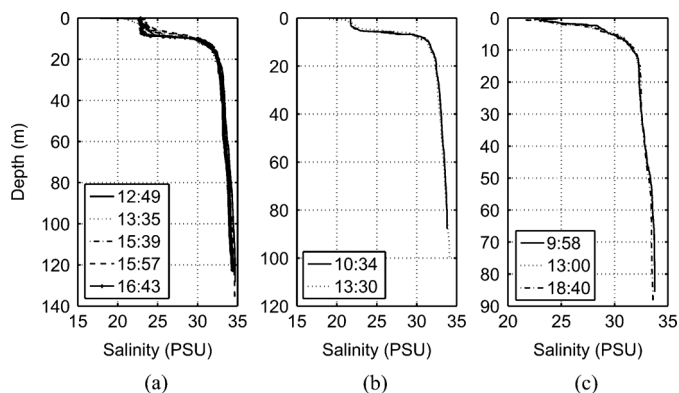


Fig. 5. Salinity profiles measured on board *R/V Gunnerus* in the Trondheim fjord on (a) May 25, 2011; (b) May 26, 2011; and (c) May 27, 2011.

IV. ENVIRONMENTAL DATA

This section describes the environment of the UAN deployment area, and reports the main environmental data gathered during the experimental activities of UAN11.

A. Bathymetry and Bottom Properties

Fig. 3 illustrates a 3-D reconstruction of the bathymetry of the experimental area, including FNO locations and conductivity–temperature–depth (CTD) casts. The STU gateway node was located at 90-m water depth, at 800 m from shore. FNO1 was positioned at about 160 m from the STU at 96-m water depth; FNO2 was deployed in a shallower area, at 39-m water depth. This node was the farthest away from the STU, at a distance of about 900 m. Finally, FNO3, a simplified node implementing the network stack up to the routing, was positioned at 98-m water depth, 400 m away from the STU.

The sediment in the region is mainly clay, whereas the underwater hills and steep regions are characterized by rock, covered with mud and clay due to the influence of rivers and tides.

B. Water Column Properties

Conductivity, temperature, and salinity data were collected several times a day, using a profiler deployed from the research vessel. Locations of the CTD casts, superimposed with the bathymetry of the area, are shown in Fig. 3. Additional CTDs were also taken farther away from the experimental area and are not displayed in the picture. Figs. 5 and 6, respectively, show the salinity profiles and the sound-speed profiles (SSPs), during three days of the experiment, between May 25 and 27, 2011, taken at various hours of the day. From Fig. 5, the presence of fresh water in the upper layers is visible, due to river run off and rain. As shown in Fig. 6, the typical SSP during the days of the sea trial was characterized by an initial negative gradient, followed by a positive gradient, with the minimum at around 40-m depth. This general behavior of the SSPs remained quite stable throughout the experiment, with the exception of May 27, 2011, when the surface layer changed (the effect of rain and wind that characterized the first days disappeared) creating a first layer with positive gradient, followed by a quasi-constant profile, and again the profile ended with the sequence of nega-

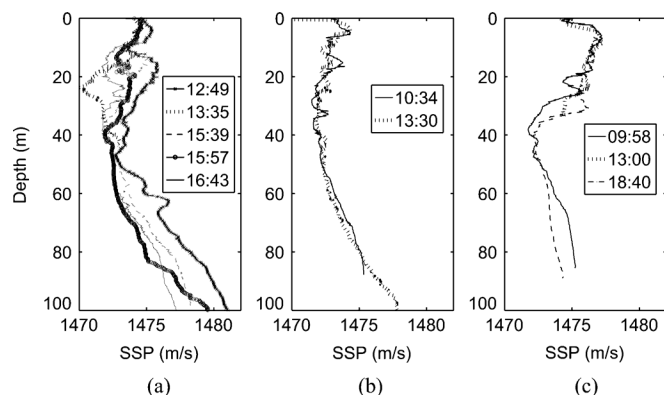


Fig. 6. SSPs measured on board *R/V Gunnerus* in the Trondheim fjord on (a) May 25, 2011; (b) May 26, 2011; and (c) May 27, 2011.

tive and positive gradients, with the minimum reached at 40-m depth.

V. COMMUNICATION PERFORMANCE

The UANp network was continuously operated during the five days of the UAN11 sea trial, from May 23 to 27, 2011. During this period, the entire network stack was fully tested, nodes were routinely added and/or removed, AUVs were seamlessly deployed within the existing fixed network, and both fixed and mobile nodes were recovered for battery recharging and then redeployed without effects on the network operation. Overall, the UANp system showed a level of robustness beyond what is normally expected in prototype equipment testing at sea. The AUVs were tested both as relay nodes, and as mobile assets of the protection system, directed acoustically from the ground C2 station, and/or moving autonomously when contact with the network was lost.

The first two days of the experiment were, for the most part, devoted to the network setup and to test the lowest levels of the UAN, from the physical transmission up to the MAC and routing layers. Between May 23 and 24, 2011, the TUN–IP layer and IS–MOOS were used in limited periods of time, mainly to test their integration with the other network components. The complete network stack was used continuously from May 25 to 27, 2011. On May 26, 2011, network security features were activated and left on until the end of the tests. The most complex network configuration was tested on May 27, 2011, when three FNOs were simultaneously in the water, together with two mobile nodes. In this case, the network was integrated within the global protection system and connected with the C2 station, which was able to receive data and send commands to the nodes/sensors.

Throughout the sea tests, the communication performance was quite variable. Usually, a 500-b/s data rate was used with success in the early hours of each day, but 200 b/s was often necessary, especially in the afternoon. To attempt to separate the effects of the acoustic channel from those of the system traffic, the performance during the sea tests has been evaluated at different layers using complementary metrics.

- The CIR, the received peak intensity, and the SINR, as directly measured by the acoustic modems, were used to characterize the physical layer operation.

TABLE I
PL AT MIDDLEWARE LEVEL PER DAY PER EACH NODE

Date	Node	Average Packet Loss (%)
23 May 2011	FNO1	0
	FNO2	29.37
24 May 2011	FNO1	11.11
25 May 2011	FNO2	58.75
26 May 2011	R/V	32.76
	FNO2	54.76
27 May 2011	Folaga1	18.31 (until 2.00 pm)
	Folaga2	49.64 (after 3.00 pm)
	R/V	40.58
	FNO2	68.38

TABLE II
RTT AT MIDDLEWARE LEVEL PER DAY PER EACH NODE

Date	Node	Average RTT (s)
23 May 2011	FNO2	17.39
25 May 2011	FNO2	58.71
26 May 2011	R/V	248.91
	FNO2	54.39
27 May 2011	Folaga1	38.81 (up to 2.00 pm)
	Folaga2	112.95 (after 3.00 pm)
	R/V	35.28
	FNO2	107.42

- The RTT and the PL were used to evaluate the upper layers of the network, the TUN–IP layer, and the MOOS middleware. The RTT has been computed as packet end-to-end delay, back and forth. The maximal RTT was estimated during flooding at the node discovery phase. Note that during this phase the upper levels of the network are not activated, so maximal RTT tends to be underestimated. This prompted for manually setting a maximal RTT timeout value of 120 s that covered most of the practical situations (see Table II). In the case of a busy channel, the node backs off for a random fraction of the RTT before verifying the availability of the channel for transmission. The PL has been computed from the number of packets successfully received at destination, over the total number of packets sent from the source.

A. Physical Layer Performance

Fig. 7 illustrates the data (CIR, peak intensity, SINR), as extracted from the modem logs in the transect between the STU and FNO2, on May 25, 2011. The contour maps shown in Fig. 7(a) were obtained using a constant false alarm ratio (CFAR) test. The CFAR test discards any peak below a threshold equal to the median of the CIR samples subtracted from the standard deviation of the thermal noise (assumed

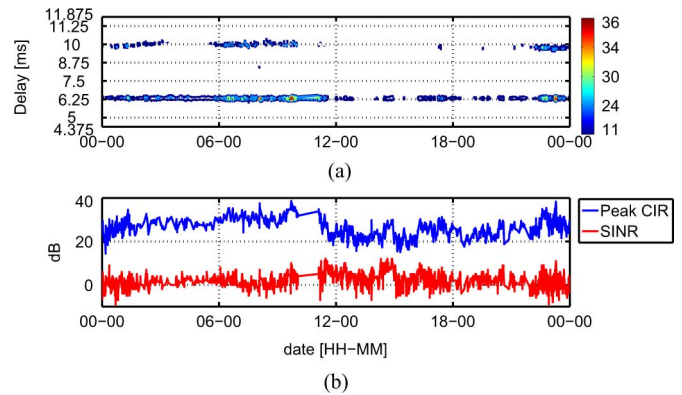


Fig. 7. Measurements of the underwater acoustic channel quality on May 25, 2011, transect FNO2–STU: (a) CIR contour map in decibels, denoised using a CFAR test (see [20] and text for details); and (b) peak CIR and SINR values in decibels.

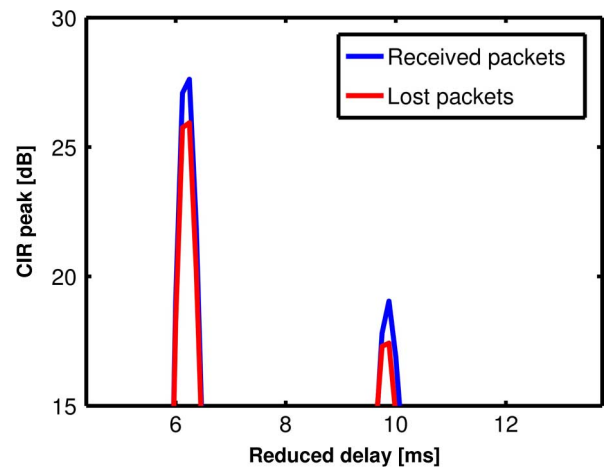


Fig. 8. Measurements of the underwater acoustic channel quality on May 25, 2011, transect FNO2–STU: the average CIR value of the main path for received packets is 1.86 dB higher than the average peak CIR in the case of lost packets.

Gaussian), and increased by a guard margin (details of the CFAR method can be found in [20]). The scales used in Figs. 7–10 are simply 16-b discrete levels shown in decibel scales with an undefined but constant reference level across figures. Note that there is a multipath effect in the acoustic channel that disappears in the central hours of the day, in correspondence with a decrease in SNR of the peak CIR curve going below 30 dB at around 12:00:00 P.M. [Fig. 7(b)]. The communication on May 25, 2011, which Fig. 7 refers to, was very variable, with periods of good communication and high reception ratio, interleaved with periods characterized by high PL. The performance deteriorated throughout the day, and from the late morning, each transmission often required several retransmissions to make the packet get through.

Statistically, the higher is the CIR main arrival, the better the communication performance, with a higher reception ratio at the receiver, even in presence of multipath. Even though the SNR was typically quite low, the average of the main path of the CIR was always higher when packets were received correctly. This is shown in Fig. 8 for May 25, 2011, with an average CIR of the main path in the case of received packets 1.86 dB higher than in the case of lost packets. This suggests that the SNR at the receiver was fluctuating above and below the threshold for correct receiving. Note also that, on May 25, 2011, the decrease in

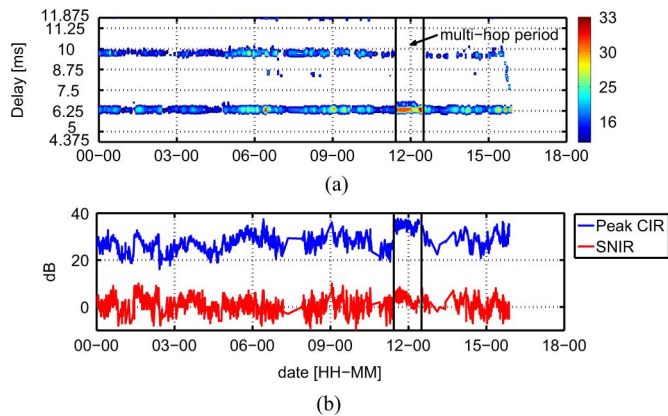


Fig. 9. Measurements of the underwater acoustic channel quality on May 26, 2011, transect FNO2-STU: (a) CIR contour map in decibels, denoised using a CFAR test (see [20] and text for details); (b) peak CIR and SNIR values in decibels. A multihop link through mobile node FNO3 was used from 11:30:00 A.M. to 12:30:00 P.M. During multihop, both the contour values in (a) and the peak CIR and SNIR in (b) are the average values of the two intermediate links (FNO2-FNO3 and FNO3-STU), showing a visible gain when compared to previous and subsequent values in the direct FNO2-STU link.

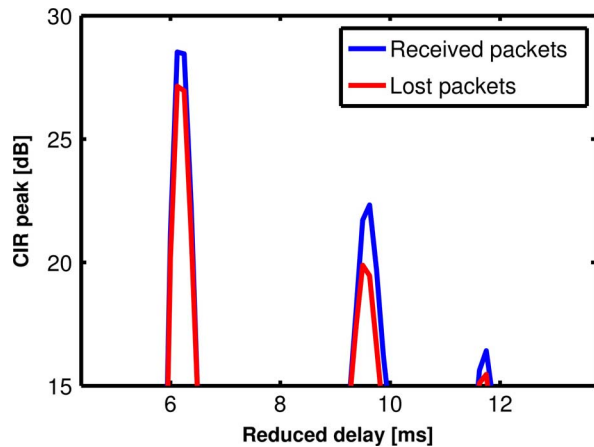


Fig. 10. Measurements of the underwater acoustic channel quality on May 26, 2011, transect FNO2-STU: the average CIR value of the main path for received packets is 1.5 dB higher than the average peak CIR in the case of lost packets.

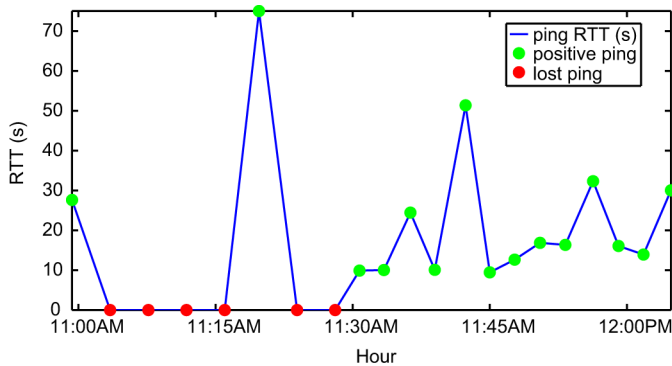


Fig. 11. RTT of pings of 20 B sent from STU to FNO2 between 11:00 A.M. and 12:00 P.M. on May 26, 2011: after a period of direct unsuccessful communication between the nodes, from 11:30:00 a.m., the communication was routed for about 1 h via FNO3. The picture shows a visible increase in the performance that corresponds to the new path.

the average CIR is less evident for the second arrival. On May 26, 2011, the same situation occurred [see Fig. 9(a)], however, from 11:30:00 A.M. to 12:30:00 P.M., the network was modified with FNO3 used as relay to reach FNO2 through a bidirectional

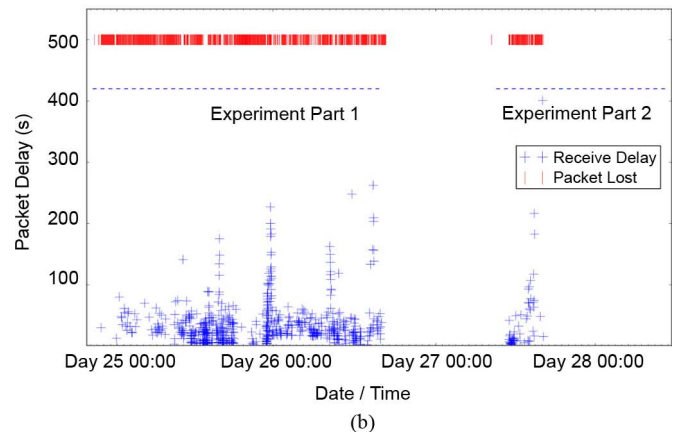
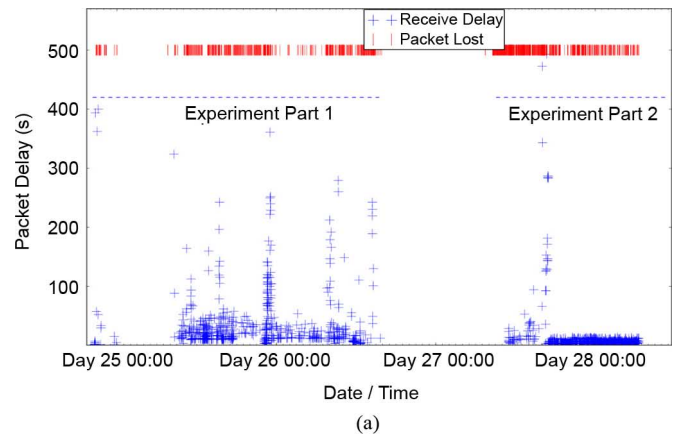


Fig. 12. Packet delays as computed at IP layer (a) from STU to FNO2 and (b) from FNO2 to STU. Total PL was 40%, from STU to FNO2, and 43%, from FNO2 to STU. Most of the data were received with a delay of up to 3–20 s. High packet delay was due to the buffering system present on the nodes.

multihop link. Everything else being equal, this had the effect of immediately improving the channel communication conditions between FNO2 and STU, as shown in the peak CIR on the upper curve of Fig. 9(b), and a subsequent degradation as soon as the multihop link was removed. It should be noted that the contour plot of Fig. 9(a) in the time interval 11:30:00 A.M. to 12:30:00 P.M. is obtained as the simple average channel response of the two intermediate links FNO3-STU and FNO2-FNO3, but that has the advantage of showing STU-FNO2 link information in a single figure for an easier analysis. The comparison between the mean CIR for received and lost packets is shown in Fig. 10, where, again, successful packets show higher multipath amplitudes when compared with the mean CIR of lost packets, which confirms that the higher the SNR, the better the communication, regardless of the presence of a period of multipaths. To better highlight the visible increase in the communication performance during the multihop period, Fig. 11 reports a sequence of successful pings executed, when FNO3 was used as a relay, within a long period of unsuccessful communication using the direct link STU-FNO2. Note that in Fig. 11, lost pings can correspond to packets that were lost in the water or to packets whose RTT exceeded the maximal RTT timeout value of 120 s. This design was necessary to force issuing the next ping request. As such, a lost ping in Fig. 11 indicates bad channel conditions, long queue backlogs, or both at the same time, since the former leads to the latter.

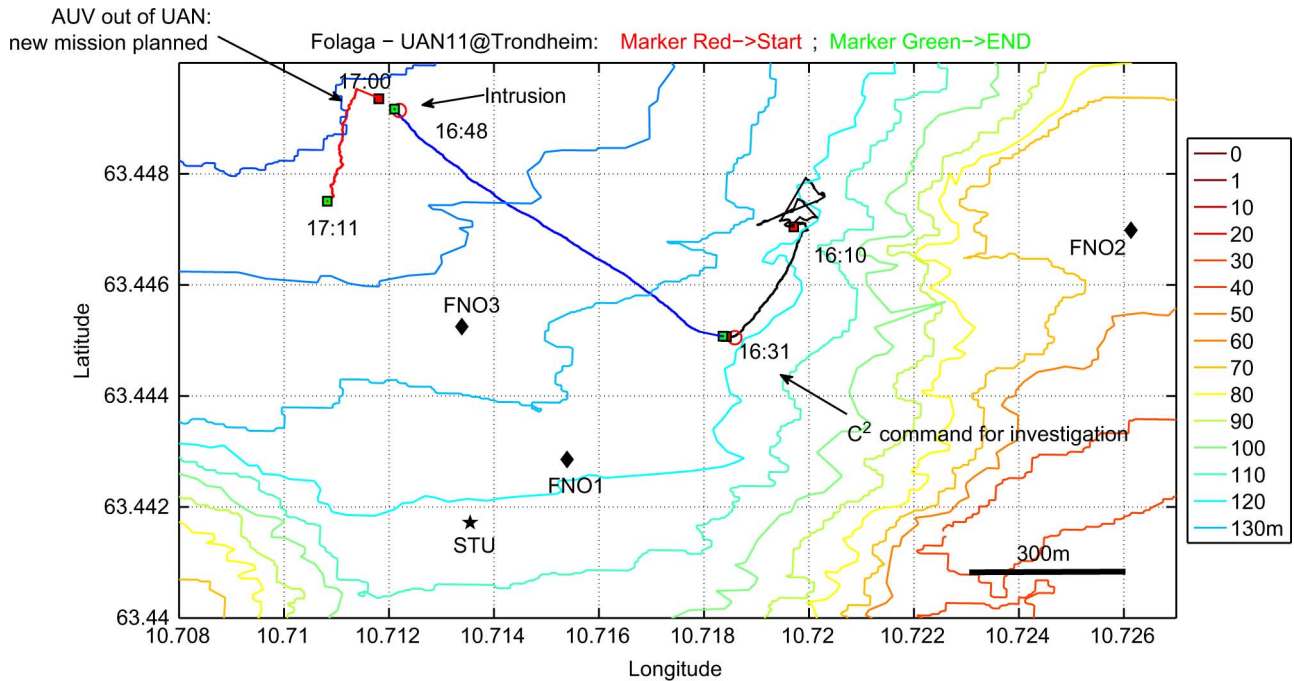


Fig. 13. e-Folaga trajectories on May 27, 2011: The vehicle was acoustically controlled by the command and control and moved to investigate a possible intrusion. The vehicle found itself without acoustic connectivity (17:00:00Z) and planned an autonomous mission to move closer to the STU (red line), where it was able to reenter into the UAN. The point of intrusion was located in the upper-left part of the picture (63.449° N, 10.712° E).

B. TUN-IP and MOOS Performance

This section analyses the performance of the upper layers of the network during the UAN11 sea trial. The TUN-IP layer represents the link between the physical layer and the upper parts of the network, i.e., transport, middleware, and applications. Hence, its performance turns out to be very important to understand the UANp performance at network level.

Fig. 12 shows the IP layer packet delay, as measured in the link between STU and FNO2 in Fig. 12(a), and between FNO2 and STU in Fig. 12(b), from May 25 to 27, 2011. This was the link where the highest number of packets was exchanged.

During the period of experimentation, observed isolated packet delays increased up to 500 s with a total PL of about 40%, from STU to FNO2, and of 43%, from FNO2 to STU. However, most of the data were received with a delay between 3 and 20 s. High packet delay was due mainly to queue backlog and buffering. It is worth pointing out that no feedback was available at the TUN-IP layer on the success of the delivery; packets would simply be discarded after being sent out to the acoustic modems via a serial line. If for any reason the remote node did not respond to specific control commands, the link was assumed as broken by the transmitter, which considered the packet as lost before reception. On several occasions, however, as came out during postprocessing after the sea trial, the remote node was indeed able to receive the incoming packet, whereas it was its reply to be lost, and never received by the first node.

Middleware performance, in terms of PL and RTT (i.e., end-to-end delay, back and forth) is summarized in Tables I and II for the period May 23–27, 2011, per each node of the network. Average PL varied between 0% and 68% approximately, remaining in most cases between 30% and 50%; average RTT went from 7 to 240 s, remaining between 60 and 120 s most of

the time. These values sum up the delays of the entire network stack, both at source and at destination. Note that, due to the loss of the node during recovery, RTT statistics for FNO1 on May 23 and 24, 2011, are not available, even though the node was operative in the period.

C. UANp Operational Example

On May 27, 2011, the most complex network was in the water. The UAN was composed of three FNOs (STU, FNO2, and FNO3) plus two mobile nodes. The network was also integrated into the protection system, composed of underwater, aerial, and terrestrial sensors, monitored and controlled by the C2 station. In this context, a complex anti-intrusion scenario was set up to verify the capability of the system to detect and respond to threats. Within this scenario, the e-Folaga AUVs were used as mobile assets of the protection system, i.e., as reactive means acoustically controlled by the C2 station to respond to intrusions, and kept mostly on surface. To this aim, when one of the FNOs detected a possible intrusion, the C2 station sent one of the AUVs to the point of intrusion to investigate the area. When the vehicle arrived to the designated point, however, it found itself out of the network, without acoustic connectivity. For this reason, after detecting the poor level of communication, the mission planner onboard the AUV, autonomously planned a new mission to move closer to the STU. Note that the vehicle was not equipped with an acoustic model able to predict its movement toward poorly covered areas, whereas the mission planner was only able to track the PL at the application level to identify when the AUV was in regions characterized by poor communication conditions. This scenario is represented in Fig. 13 in terms of the trajectories followed by the AUV during its mission. The picture also reports the main mission phases.

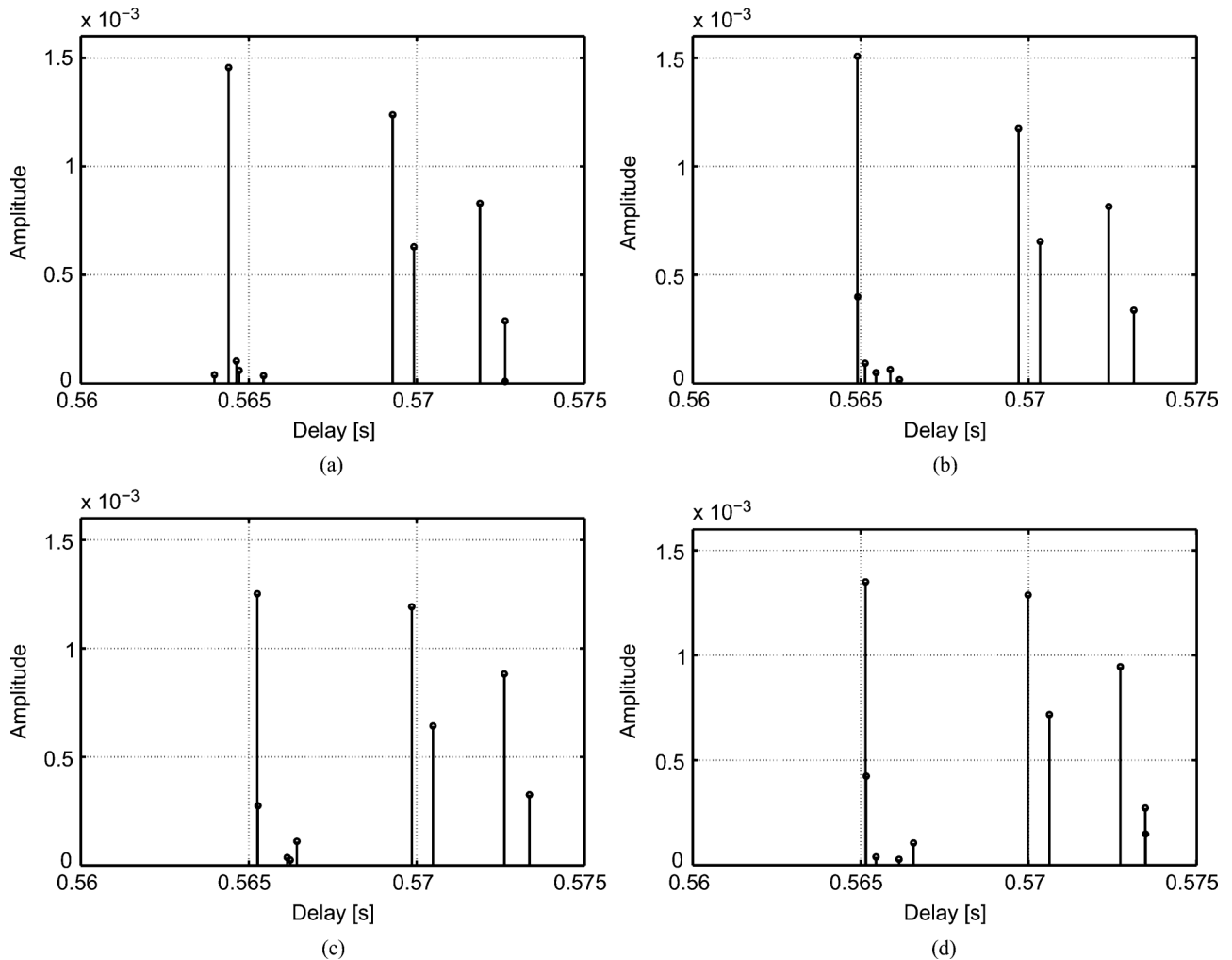


Fig. 14. Evolution of the CIR between STU (source) at 80-m depth and FNO2 (receiver) at 40-m depth, as calculated by Bellhop with varying SSPs on May 25, 2011: (a) at 9:50:00Z; (b) at 14:26:00Z; (c) at 15:43:00Z; and (d) at 16:34:00Z. The decrease of the main paths after 15:43:00Z is visible when comparing plots (c) and (d) with plots (a) and (b).

VI. ACOUSTIC PROPAGATION AT UAN11

To test if indeed there was a degradation in channel communication performance due to the variation in the environmental conditions (i.e., the SSP), the Bellhop ray model was run in correspondence with the SSP as measured during each day.

The numerical simulation has been performed by computing the main path impulse response and the incoherent transmission loss (TL) to analyze the results of the sea trial

$$TL(r, r_s) = -20 \text{Log}_{10} \left| \frac{p^{(I)}(r, z)}{p_0(r_s)} \right| \quad (1)$$

where the incoherent pressure field $p^{(I)}$ is computed as

$$p^{(I)}(r, z) = \left[\sum_{j=1}^{N(r, z)} |p_j(r, z)|^2 \right]^{1/2} \quad (2)$$

where r is the horizontal distance, z is the depth, $N(r, z)$ denotes the number of eigenrays contributing to the field at a particular receiver position, $p_j(r, z)$ is the pressure due to eigenray j , and $p_0(r_s)$ is the pressure produced at a distance of 1 m from the same source in an infinite, homogeneous medium [21].

Equation (1) is used here to assess in a qualitative way the relative variation of SNR in the channel, as the TL is linked to the SNR through the well-known sonar equation [21]

$$\text{SNR} = \text{SL} - \text{TL} - (N + \text{RL}) \quad (3)$$

where SL is the source level, N is the ambient noise level, and RL is the reverberation level.

In what follows we give more emphasis on the analysis of May 25, 2011, when the largest number of CTDs was taken within the same day, permitting to have a better picture of the changes in the TL as the environment changed. Further simulations have been performed on May 27, 2011, for the acoustic links between the STU and the mobile nodes, and their results are also reported.

A. Changes in CIR and TL Between STU and FNO2 on May 25, 2011

The variation of the CIR and of the incoherent TL, as computed by Bellhop, with varying SSPs, on May 25, 2011, and for the transect between STU (source) and FNO2 (receiver), is reported in Figs. 14 and 15, respectively. The model indeed predicts a decrease in the intensity of the main arrivals (Fig. 14) and

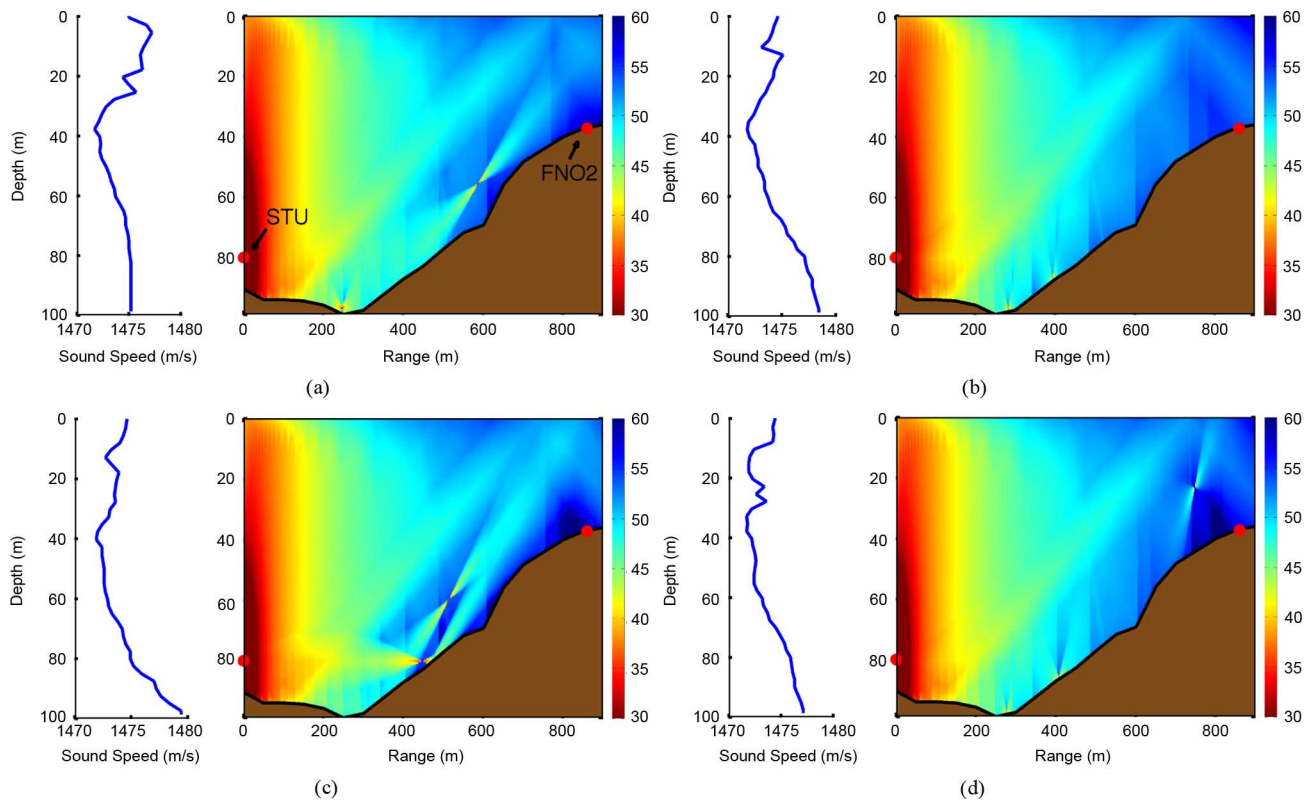


Fig. 15. Evolution of the incoherent TL, as calculated by Bellhop with varying SSPs at various hours of May 25, 2011: (a) at 9:50:00Z; (b) at 14:26:00Z; (c) at 15:43:00Z; and (d) at 16:34:00Z. STU (source) is at 80-m depth, and FNO2 (receiver) is located at 40-m depth. Both nodes are represented as red circles at the corresponding depths. Note, however, that the positions indicated by the circles are only indicative of the true positions of the nodes in the water.

a consequent increase in the TL at FNO2 developing within the day (Fig. 15), accompanying the communication performance as observed in the experimental data. Note that the CIR and the TL shown in Fig. 14 are used as an indication of qualitative variation of the response of the acoustic channel and are not meant to be numerically compared with field values. It is also worth pointing out that the absolute delay values in Fig. 14 do not correspond to those measured in the field due to a time normalization executed by the acoustic modems before recording the CIR. However, the time difference between the first and second main peaks in the computed CIR is compatible with those measured in the field, taking into account the uncertainty (greater than 1 m) in the localization of the nodes. The variation in the communication channel is due to the afternoon change in the SSP, with the presence of a higher gradient in the lowest part of the profile. This variation modifies the TL pattern, moving an important part of the energy upwards, and hence away from the receiver (FNO2), determining a corresponding increase in the TL, and a decrease in the received signal. This is shown in Fig. 15 as a TL increase of at least 5 dB at the FNO2 position from morning conditions [Fig. 15(a) and (b)] to the development of a shadow zone later in the day [Fig. 15(c) and (d)]. Due to the localized nature of that shadow zone and normal uncertainty on node position, model predictions should be taken with the usual care and more as an indication of tendency, rather than as actual TL values.

To better highlight this difference in the TL at the FNO2 location, Fig. 16 reports, on the left, the TL values saturated between 50 and 55 dB and corresponding to the SSP variations,

and on the right, the corresponding ray paths. The figures show the energy bounced off the bottom away from the FNO2. This kind of slight change in the lower portion of the SSP has been registered often in the afternoon during the sea tests, and it was usually accompanied by a rapid deterioration in the communication performance between STU and FNO2. There was no further CTD available after 16:34:00Z, and this lack of information prevented the attempt of modeling the observed performance recovery after 17:30:00Z. The predicted CIR shows a decrease in the first arrival energy, while the second main arrival does not show a significant variation. While there is discrepancy between the relative amplitudes of the first and second arrivals, as predicted by BELLHOP and as measured in the field, the model is able to predict the trend of variation of both first and second arrivals, as seen in the experimental data. The variation in the TL due to the afternoon change in the SSP appears also at shorter distances, as in the case between STU and FNO1, which are less than 200 m apart. However, at such distances, where the SNR is in any case well above the reception threshold, small variations in TL are not critical to influence the overall ability to communicate. In these conditions, the impact of the network itself (e.g., MAC, multihops, etc.) possibly justifies the variation in the communication performance.

As a final case, the anti-intrusion scenario described in the previous section and in Fig. 13, and tested on May 27, 2011, has been simulated with Bellhop to evaluate the incoherent TL corresponding to the two phases of the AUV mission: 1) before receiving the command from the C2 station; and 2) once it reached the intrusion point. Fig. 17 shows the results obtained in

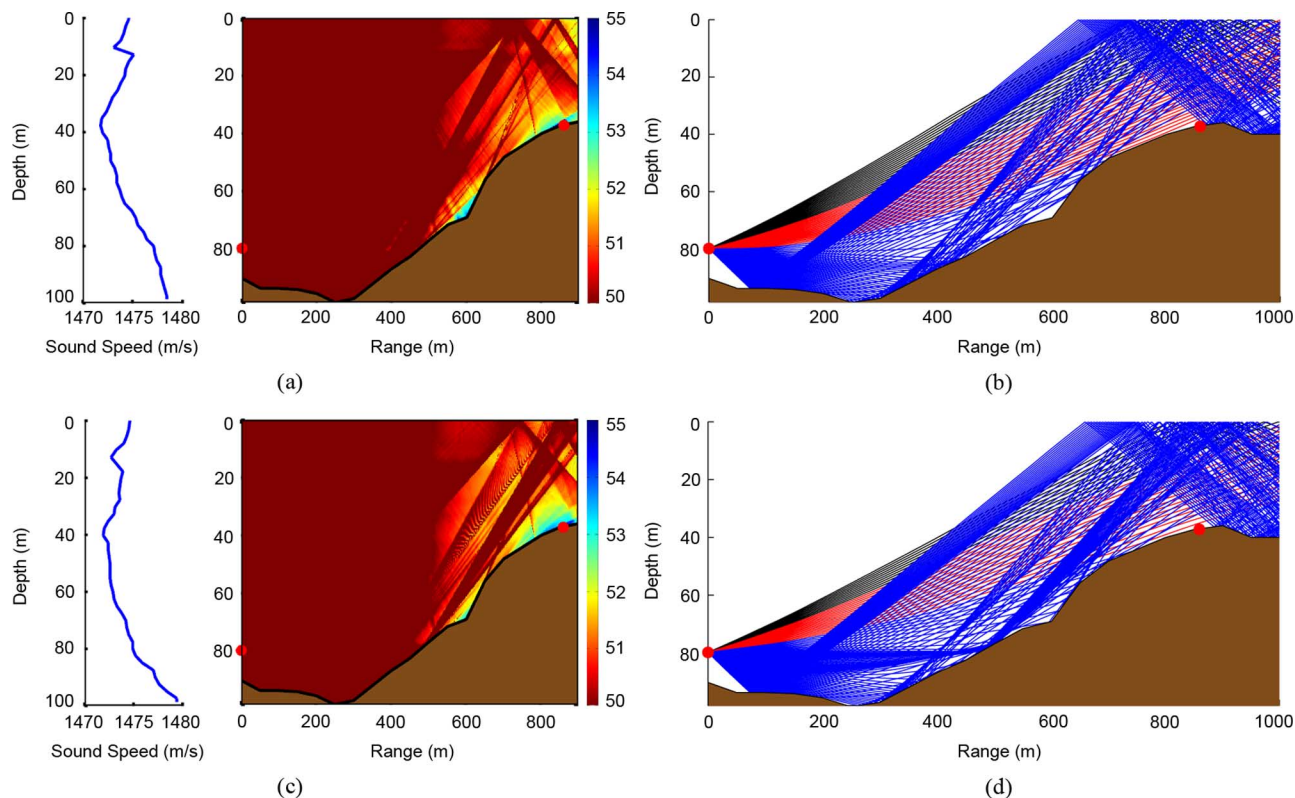


Fig. 16. Left: Incoherent transmission loss saturated between 50 and 55 dB to highlight its variation at the FNO2 location. The variation is due to the change in the SSP on May 25, 2011: (a) at 14:26:00Z; and (c) at 15:43:00Z. The positions of the transmitter and the receiver are indicated by red circles. Right: Ray paths in the transect between STU and FNO2: (b) at 14:26:00Z; and (d) at 15:43:00Z. Note that due to the bathymetry no direct path exists between the source and the receiver.

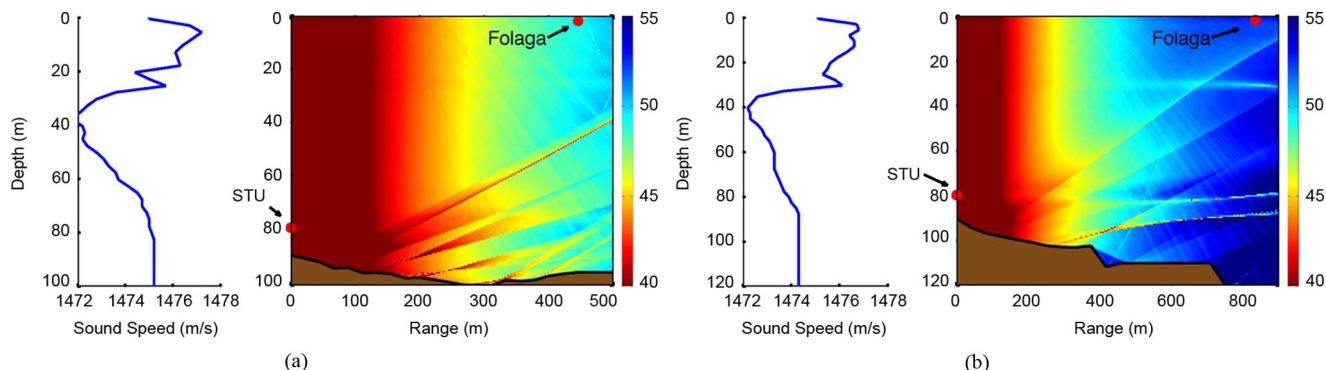


Fig. 17. TL between STU and the Folaga on May 27, 2011: (a) at 16:00:00Z and (b) at 18:00:00Z when the vehicle found itself out of the network. The difference in TL between the two cases is about 6 dB (both nodes are represented as red circles).

the two cases. The distance from STU, together with the change in bathymetry, resulted in an important increase in the TL (of about 6 dB) and the consequent degradation of the communication.

VII. OBSERVATIONS AND REMARKS

On the basis of the presented results, several comments can be made on the network performance at different levels.

- The acoustic modems used in the UANp operations appeared to be quite robust against the multipath structure found in the UAN11 sea trial. In the UAN11 scenario, where the main arrival was well separated, the KM modems were effectively able to exploit their online computation of the CIR to mitigate multipaths effects, increasing the probability to correctly receive a packet. On the contrary, they seemed more fragile with respect

to SNR decrease. Trondheim Fjord acoustic communication conditions were difficult throughout the days of the experiment, with a fairly low SNR (less than 10 dB). In these conditions, even small variations of the SNR implied significant changes in the communication capabilities.

- The large delays experienced at the upper levels of the network cannot only be caused by the packet propagation in the water, while several concurrent effects were interacting in producing such performance. First, if a packet was lost in the water channel due to noise, collisions, or signal fade, the acoustic modems would attempt retransmission up to three times before stopping any further attempt with that packet. Furthermore, the average size of a MOOS packet was 150 B, which is above the maximum size to be transmitted by the acoustic modem as a single acoustic telegram, for the fastest 500-b/s bitrate used during the sea trial

(see Section II-A1). As a result, MOOS packets were often fragmented into several frames, each one transmitted separately and with its own acknowledgment and, if necessary, retransmission. As explained above, the maximum number of attempts per telegram was set to three, which in case of successive failure implied telegram discard and PL.

- In the case of smaller packets, as ping packets (see Fig. 11), large delays were mostly due to queue backlog, as in the case of new ping packets fed into the system before the former was finished, or in the case of MOOS data traffic simultaneously present with ping traffic. Other delays might also have been caused by the operation of the CSMA/CA protocol. According to this protocol, each node is able to detect a busy channel (i.e., another node is already transmitting) to prevent collisions. In this case, the node backs off for a random fraction of the RTT, before verifying the availability of the channel for transmission. However, in the presence of high propagation delays, typical of underwater acoustic networks, one device might not detect that another one has already started the transmission, resulting in a simultaneous transmission and a collision. This might become even more important in the case of multihop connections, when the packets have to travel through more than one link to get to their destinations. As a result, the overall network performance, including IP, was strongly related to the acoustic channel conditions, i.e., relative locations between the nodes, mobile nodes movement, and to the particular traffic which was undergoing into the network layers, as, for example, in situations of network congestion.
- Previous work on P2P communications in the presence of environmental variability has shown a decrease of signal coherence, and associated loss of performance, due to surface agitation [22], water column thermal activity [23], and the influence of internal waves [24]. In another case, it was reported that surface agitation contributed to a mixing of the ocean upper layer, effectively contributing to ameliorate the acoustic propagation conditions on a channel near the bottom, where both the source and the receiver were located [25]. The latter case is in generic agreement with the situation reported in this paper where the computation of the TL and of the CIR estimate is in agreement with the communication performance observed in the field, at least in a qualitative manner. In the UANp scenario, the communication was dominated by the SNR, and in this case, the TL seems to be a good indicator of performance variations. Even though it is clear that the overall performance of the network depends on the interplay occurring at different layers, the use of the TL or similar channel indicators can provide useful information that can be effectively used to adapt the behavior even at the highest levels of the network.

VIII. CONCLUSION

This work analyzed the performance of a UAN composed of four FNOs and three mobile nodes. This setup was deployed during the UAN11 experimental activities held in May 2011, off

the coast of Trondheim, Norway, and was continuously operated for five days, as an integrating part of a global protection system.

This paper reports the details of the communication and network protocols employed as well as the observed field behavior, pointing out the relationship between the various network layers in explaining the overall communication performance results. Results of the experimental activities are reported using different metrics at different layers: the physical layer performance is reported in terms of CIR, received peak intensity, and SINR, as measured online by the acoustic modems; the network upper layers performance is characterized in terms of probability of PL and RTT.

The network communication was affected by the changes in the acoustic channel, and by the network structure itself, e.g., the MAC protocol, multihops, etc. In the conditions of the UAN11 sea trial, variation in the SNR appears to be more important in explaining the changes in the communication performance. The receivers could cope with the experienced multipath, exploiting their own ability in estimating the CIR, but were more fragile with respect to SNR fluctuations. Furthermore, the influence of the acoustic channel on the network appears to be more important on longer distances, where the usage of multihops to guarantee connection showed a clear increase in performance.

Environmental channel modeling with TL and CIR estimates computed with Bellhop ray-tracing code indicates that TL computation by standard methods can qualitatively predict relative variations in the communication performance. It is underlined that Bellhop predictions are qualitatively in agreement with the observed communication performances. This indicates, that, at least in the cases where the communication performance is dominated by SNR, the computation of the TL with standard ray models can be used as a relative indicator of performance variation.

Even though the network performance was indeed dependent on several concurrent effects, spread out at various network levels, it appears that the use of the TL, together with other communication performance indicators might give insights that can be useful even at the highest levels of the network. In particular, the presence of mobile nodes was useful to modify the geometry of the network on the fly and in response to online needs. In the UAN11 setting, the availability of a multihop routing layer was certainly an added value, permitting to reestablish acoustic connectivity between two nodes when a direct link was not enough. On the other side of the spectrum, the challenging communication conditions experienced during the UAN11 sea trial brought other network components to their operative limit. The CSMA MAC layer often showed its weak side: constantly requiring permission for transmissions limited collisions but added a significant overhead in a high-delay scenario.

The presence of a centralized C2 station suggested, in the design phase, the implementation of star-shaped structures throughout the network stack (flood-based routing, IP, and MOOS levels). Although the impact of such centralized schemes did not add a significant communication overhead, it did not reduce it either. In scenarios characterized by communication unreliability and extremely limited bandwidth, different approaches might lead to better efficiency: selecting the information going to the C2 station or to a master node,

and leaving more space for node autonomy, and distributed decisions at all levels can significantly reduce the overhead, improving the network's overall performance.

ACKNOWLEDGMENT

The authors would like to thank the *R/V Gunnerus* captain and crew for their support during the UAN11 experimental activities, and the entire UAN project team.

REFERENCES

- [1] J. Heidemann, M. Stojanovic, and M. Zorzi, "Underwater sensor networks: Applications, advances, and challenges," *Phil. Trans. R. Soc. A*, vol. 370, no. 1958, pp. 158–175, May 2012.
- [2] S. Petillo, H. Schmidt, and A. Balasuriya, "Constructing a distributed AUV network for underwater plume-tracking operations," *Int. J. Distrib. Sens. Netw.*, 2012, Article ID 191235.
- [3] I. F. Akyildiz, D. Pompili, and T. Melodia, "Underwater acoustic sensor networks: research challenges," *Ad Hoc Netw.*, vol. 3, no. 3, pp. 257–279, May 2005.
- [4] J. Heidemann, U. Mitra, J. Preisig, M. Stojanovic, M. Zorzi, and L. Cimini, "Guest editorial—Underwater wireless communication networks," *IEEE J. Sel. Areas Commun.*, vol. 26, no. 9, pp. 1617–1619, Jul. 2008.
- [5] M. Chitre, S. Shahabudeen, L. Freitag, and M. Sjtanovic, "Recent advances in underwater acoustic communications & networking," in *Proc. IEEE OCEANS Conf.*, 2008, DOI: 10.1109/OCEANS.2008.5152045.
- [6] D. Pompili and I. F. Akyildiz, "Overview of networking protocols for underwater wireless communications," *IEEE Commun. Mag.*, vol. 47, no. 1, pp. 97–102, Jan. 2009.
- [7] J. Rice, "SeaWeb acoustic communication and navigation networks," in *Proc. Int. Conf. Underwater Acoust. Meas., Technol. Results*, Heraklion, Crete, Greece, 2005 [Online]. Available: <http://www.uam-conferences.org/index.php/archive-past-uam-proceedings>
- [8] L. Freitag, M. Grund, S. Singh, J. Partan, P. Koski, and K. Ball, "The WHOI micro-modem: An acoustic communications and navigation system for multiple platforms," in *Proc. MTS/IEEE OCEANS Conf.*, 2005, pp. 1086–1092.
- [9] T. Schneider and H. Schmidt, "Unified command and control for heterogeneous marine sensing networks," *J. Field Robot.*, vol. 27, no. 6, pp. 876–889, 2010.
- [10] C. Petrioli, R. Petroccia, and J. R. Potter, "Performance evaluation of underwater MAC protocols: from simulation to at-sea testing," in *Proc. IEEE OCEANS Conf.*, Santander, Spain, 2011, DOI: 10.1109/Oceans-Spain.2011.6003479.
- [11] A. Caiti, V. Calabro, G. Dini, A. L. Duca, and A. Munafò, "Secure cooperation of autonomous mobile sensors using an underwater acoustic network," *Sensors*, vol. 12, no. 2, pp. 1967–1989, Feb. 2012.
- [12] A. Caiti, T. Husoy, S. M. Jesus, I. Karasalo, R. Massimelli, A. Munafò, T. A. Reinen, and A. Silva, "Underwater acoustic networks: The Fp7 UAN project," in *Proc. 9th IFAC Conf. Manoeuv. Control Marine Craft*, Jul. 2012, pp. 1–6.
- [13] F. Zabel, C. Martins, and A. Silva, "Design of a UAN node capable of high-data rate transmission," *Sea Technol.*, vol. 52, no. 3, pp. 32–36, Mar. 2011.
- [14] A. Caiti, V. Calabrò, G. Dini, A. L. Duca, and A. Munafò, "Mobile underwater sensor networks for protection and security: field experience at the UAN11 experiment," *J. Field Robot.*, vol. 30, no. 2, pp. 237–253, 2013.
- [15] M. B. Porter, "The BELLHOP manual and user's guide," Tech. Rep., 2011.
- [16] T. Husoy, M. Pettersen, B. Nilsson, T. Öberg, N. Warakagoda, and A. Lie, "Implementation of an underwater acoustic modem with network capability," in *Proc. IEEE OCEANS Conf.*, Apr. 2011, DOI: 10.1109/Oceans-Spain.2011.6003642.
- [17] Kongsberg Maritime AS, "cNODE mini transponder instruction manual," Tech. Rep., Mar. 2011.
- [18] U. Vilaipornsawai, A. Silva, and S. Jesus, "Underwater communications for moving source using geometry-adapted time reversal and DFE: UAN10 data," in *Proc. IEEE OCEANS Conf.*, Apr. 2011, DOI: 10.1109/Oceans-Spain.2011.6003513.

- [19] Oxford Mobile Robotics Group, "The MOOS cross platform software for robotics research," Tech. Rep., Dec. 2011.
- [20] E. Sousa, V. Jovanović, and C. Daigneault, "Delay spread measurements for the digital cellular channel in Toronto," *IEEE Trans. Veh. Tech.*, vol. 43, no. 4, pp. 837–847, Nov. 1994.
- [21] F. B. Jensen, W. A. Kuperman, M. Porter, and H. Schmidt, *Computational Ocean Acoustics*, R. T. Beyer, Ed. New York, NY, USA: Springer-Verlag, 1994, ch. 3.
- [22] M. Badiey, Y. Mu, J. Simmen, and S. Forsythe, "Signal variability in shallow-water sound channels," *IEEE J. Ocean. Eng.*, vol. 25, no. 4, pp. 492–500, Oct. 2000.
- [23] N. Carbone and W. Hodgkiss, "Effects of tidally driven temperature fluctuations on shallow-water acoustic communications at 18 kHz," *IEEE J. Ocean. Eng.*, vol. 25, no. 1, pp. 84–94, Jan. 2000.
- [24] A. Song, M. Badiey, A. Newhall, J. Lynch, and H. Deferrari, "Effects of internal waves on acoustic coherent communications during SW06," in *Proc. Eur. Conf. Underwater Acoust.*, Paris, France, Jun. 2008, pp. 286–290.
- [25] A. Song, M. Badiey, H. Song, W. Hodgkiss, M. Porter, and K. Group, "Impact of ocean variability on coherent underwater acoustic communications during the Kauai experiment (KauaiEx)," *J. Acoust. Soc. Amer.*, vol. 123, no. 2, pp. 856–865, Feb. 2008.



Andrea Caiti (M'92–SM'04) was born in Naples, Italy, in 1963. He received the M.S. degree in electronic engineering from the University of Genoa, Genoa, Italy, in 1988.

Since 2007, he has been a Full Professor of Automatic Control at the University of Pisa, Pisa, Italy, teaching courses on automatic control (both in Pisa and at the Naval Academy in Leghorn), system identification, and underwater systems. He has previously held positions as a Staff Scientist at the NATO SACLANT Undersea Research Center [currently Center for Maritime Research and Experimentation (CMRE), La Spezia, Italy; 1989–1994]; an Adjunct Professor at the University of Genoa (1995–1996); an Assistant Professor at the University of Pisa (1996–1998); an Associate Professor at the Universities of Siena, Siena, Italy (1998–2001); and an Associate Professor at the University of Pisa (2001–2007). He was the Director of the Interuniversity Research Centre on Integrated Systems for the Marine Environment (ISME; 2001–2008), and is currently Coordinator of the Ph.D. Programme in Automation Robotics and Bioengineering at the University of Pisa. His current research interests are focused on underwater acoustics and marine robotics, automation in oceanography, nonlinear systems analysis, control, and optimization.



Knut Grythe (M'85) received the M.Sc. degree in electrical engineering from the Norwegian University of Technology (NTNU), Trondheim, Norway, in 1974.

After four years in the industry, he joined SINTEF, Trondheim, Norway, in 1980. After a two-years scholarship at NTNU in 1984–1986, he returned to SINTEF as a Senior Scientist. He has been involved in many national and international projects. His research interests include radio and underwater communication systems, signal processing, and

information theory.



Jens M. Hovem received the Ph.D. degree in communication theory from the Norwegian University of Science and Technology (NTNU), Trondheim, Norway, in 1966.

His experience includes two periods at SACLANT Undersea Research Centre [now Center for Maritime Research and Experimentation (CMRE), La Spezia, Italy], as a Scientist and Division Chief. In 1991, he was appointed Professor at the Department of Electronics and Telecommunication, NTNU, conducting research and giving courses in underwater acoustics and signal processing. He has been a Visiting Scientist at the Applied Research Laboratories (ARL), The University of Texas at Austin, Austin, TX, USA, in

1979 and 2002, and at CNRS Laboratoire de Mécanique et d'Acoustique, Marseilles, France, in 1998. He is now Professor Emeritus at the Department of Electronics and Telecommunication, NTNU, and also works as an independent consultant in underwater acoustic. His main fields of interest are underwater acoustics and signal processing.



Sérgio M. Jesus (M'09) received the "Doctorat es-Sciences" degree in engineering sciences from the University of Nice, Nice, France, in 1986.

From 1985 to 1992, he was a Staff Scientist at the SACLANT Undersea Research Centre [NURC, currently Center for Maritime Research and Experimentation (CMRE)], La Spezia, Italy. During that period, he was involved with underwater acoustic field noise directionality and early studies on target detection using matched field processing. In 1992, he joined the Electronics and Computation Department,

University of Algarve, Faro, Portugal, where he is currently Full Professor. His interests are underwater acoustic array signal processing, model-based inversion, underwater communications, as well as other aspects dealing with sound propagation in the ocean, including its usage for environmental and biodiversity monitoring and conservation.

Prof. Jesus is a member of the IEEE Signal Processing Society, the European Association for Signal Processing (EURASIP), and the Acoustical Society of America.



Arne Lie received the M.Sc. degree in electrical engineering and the Ph.D. degree in telematics from the Norwegian University of Technology (NTNU), Trondheim, Norway, in 1989 and 2008, respectively.

He is currently a Senior Scientist with SINTEF, Trondheim, Norway, where he has been employed since 1990. His research interests include wired and wireless communication, IP and custom protocol design and testing, with main application fields being powerline communication and underwater communication.



Andrea Munafó (M'09) received the B.Sc. degree in computer science engineering, the M.Sc. degree in automation engineering, and the Ph.D. degree in automation, robotics, and bioengineering from the University of Pisa, Pisa, Italy, in 2002, 2005, and 2009, respectively.

He worked as a Postdoctoral Student at the Inter-university Center on Integrated Systems for the Marine Environment, University of Pisa, from 2009 to 2013. He is currently a Research Scientist at the NATO STO Center for Maritime Research

and Experimentation (CMRE), La Spezia, Italy. His main research interests span over underwater communication, multiagent cooperation, and underwater localization.

Dr. Munafó is a member of the IEEE Oceanic Engineering Society and the IEEE Robotics and Automation Society.



Tor Arne Reinen received the M.Sc. degree in electrical engineering and the Ph.D. degree in electrical engineering and telecommunications from the Norwegian University of Technology (NTNU), Trondheim, Norway, in 1982 and 1996, respectively.

After a one-year position as a Research Assistant at NTNU in 1983, he has been a Scientist and now Senior Scientist with SINTEF, Trondheim, Norway. His research interests include physical and technical acoustics, physical modeling, and signal processing, with main focus on ultrasound and underwater acous-

tics.



António Silva received the Ph.D. degree in electrical and computer engineering from the Technical University of Lisbon, Lisbon, Portugal, in 2009.

Currently, he is a Professor at the University of Algarve, Faro, Portugal. Since 2002, he has split his time between researching physical-model-based underwater communications and developing underwater telemetry systems.



Friedrich Zabel received the B.Sc. degree in systems engineering from the University of Algarve, Faro, Portugal, in 2005.

Over the past nine years, he has designed and developed various systems for the Signal Processing Laboratory (SiPLAB), University of Algarve, and MarSensing Lda, Faro, Portugal, with applications in underwater acoustic research. His research and development interests include embedded devices and networks in underwater acoustics.